THREE-DIMENSIONAL PRINTING OF POLYVINYLIDENE FLUORIDE NANOCOMPOSITES

Sampada Bodkhe[1], Frederick P Gosselin, and Daniel Therriault[1]*

Laboratory of Multi-scale Mechanics, Department of Mechanical Engineering
[1]Research Center for High Performance Polymer and Composite Systems (CREPEC)
Ecole Polytechnique de Montreal
C.P. 6079, succ. Centre-Ville, Montreal, QC H3C 3A7, Canada
*Email: daniel.therriault@polymtl.ca

Keywords: 3D printing, Barium titanate, Multi-walled carbon nanotubes, Piezoelectric, Polyvinylidene fluoride

ABSTRACT

Piezoelectric sensors are widely used to measure temperature, pressure, flow-rate or proximity due to their high sensitivity and self-powering capability. Currently, the fabrication processes used for the piezoelectric sensors are limited to 2D film or strip configurations. Here, we present a novel fabrication approach to create piezoelectric polyvinylidene fluoride (PVDF) – barium titanate ($BaTiO_3$) nanocomposite sensors by solvent-cast 3D printing. Solvent-cast 3D printing consists of robotically-controlled deposition of polymer solutions followed by quick evaporation of the volatile solvent in order to build 3D structures. Addition of nanofillers is a proven method to significantly improve the piezoelectric properties of PVDF; $BatiO_3$ nanoparticles being new in the list of fillers are being compared with the long studied multi-walled carbon nanotubes. Our desired sensor film is obtained in a single step by extruding a solution of the PVDF nanocomposite under tailored pressures directly on the structure at the desired sensing location. The precise printing of polymer solution requires optimization of various process parameters: concentration of nanoparticles, viscosity of the solution, deposition speed and extrusion pressure. The effects of these parameters on the printing efficiency are studied using process-viscosity characterizations while their effects on the material properties are analysed using physical (i.e., XRD, FTIR) as well as piezoelectric characterization techniques. A dielectric constant of 20 and capacitance of 79 pF is obtained with a 85 µm thick barium titanate nanoparticles/PVDF composite film. FESEM is used to evaluate the morphology of the 3D printed films. Fibers (1D), films, membranes (2D) and scaffolds (3D) are further fabricated to demonstrate the flexibility of the process. These 3D printed sensors will find applications in aerospace and automotive industries for structural health monitoring.

1 INTRODUCTION

Polyvinylidene fluoride (PVDF), a semi crystalline fluoropolymer, consists of five crystalline polymorphs (also known as phases or crystal structures) – α, β, ϒ, δ and ε as discovered by Lando *et al.* [1] in 1968. Its chemical structure consists of polymer chains of repeating CF_2-CH_2 units. The spatial arrangement of the fluorine and hydrogen atoms about the C-C backbone defines the phase of PVDF. The most stable α polymorph consists of a trans-gauche (TGTG') configuration, and the piezoelectric β is found in an all trans (TTTT) planar zig-zag form [2]. As PVDF naturally crystallizes in its α-phase, the attainment of β-phase requires a physical transformation and its retention. Application of high electric fields for long duration has proved highly effective in the formation of β-phase [3, 4]. Annealing [5], electrospinning [6, 7], and stretching [8] have also shown promising results in improving β-phase. In addition, fillers (e.g., carbon nanotubes [9, 10], clay [11], cellulose [12], magnetic [13] and piezoelectric nanoparticles [14]) can be incorporated into PVDF matrix via

ultrasonication [15] or mechanical stirring [16] for β-phase retention. These fillers bearing heavy molecular chains adhere to the polar crystallites in PVDF and prevent their disorientation. Electrospinning of PVDF with 1 wt.% $BaTiO_3$ nanoparticles (BTNs), upon treatment with 3 wt.% tetra iso-pentyl ammonium chloride (TIPAC), resulted in up to 100% β-phase [17].

Multi-walled carbon nanotubes (MWCNTs) were demonstrated to be efficient in attaining higher piezoelectric properties in PVDF [18]. Electrospinning small amounts (~1.2wt.%) of MWCNTs with PVDF enhanced the piezoelectric properties by increasing the β-phase and also the flexibility of the composite [19]. Yu *et al.* [20] obtained output voltages close to 6 V upon periodically bending the nanofiber mats (electrospun with 5wt.%, MWCNTs in PVDF) with a horizontal displacement of 3 cm (initial length = 8 cm) at a bending frequency of 0.8 Hz.

The most common processes used for the fabrication of PVDF films from its solutions include solution casting [21], spin coating [5] and electrospinning [22]. While solution casting and spin coating entail further post processing like poling to attain the β-phase, electrospinning comprises of in situ poling of the fibers during their deposition. Near field electrospinning (NFES) is a process similar to 3D printing that has been successful in printing PVDF/MWCNT nanofibers and nanofiber mats [23]. NFES is the modification over conventional electrospinning process achieved by the reduction in the distance between the nozzle and the collector to obtain control over the orientation of the fibers. Here, the application of an additional electrode as collector facilitates unidirectional fiber fabrication. The oppositely charged collector electrodes aid the deposition of the fibers with oriented dipoles. The NFES technique [23] was further used to successfully fabricate PVDF fiber with 2.6 μm diameter and 500 μm length for piezoelectric actuation [24].

Solvent-cast 3D printing comes in with the advantages of fabricating structures from polymer solutions at room temperature [25]. This novel technique has proven successful in 3D printing self-supporting and free-standing structures of polymers and their functional nanocomposites. The printable materials are presently restricted to the polymer polylactide and its nanocomposites [26].

Here, we propose to use solvent-cast 3D printing to fabricate piezoelectric devices using PVDF and its nanocomposites with MWCNTs and BTNs. MWCNTs were chosen because of their well-known capability of improving the piezoelectric properties while BTNs were chosen owing to their inherent piezoelectric nature to serve as an additional contribution to PVDF's piezoelectric properties. Three different concentrations of MWCNTs in PVDF were studied and the best concentration was compared with its BTN/PVDF counterpart. A detailed study of the printing parameters and their effect on the properties of PVDF was carried out.

2 EXPERIMENTAL SECTION

2.1 Materials

PVDF (M_w ~ 534,000) and dimethyl sulfoxide (DMSO) were purchased from Sigma Aldrich. Spherical barium titanate nanoparticles (BTNs, 99.9% purity, 100 nm) were procured from Nanostructured & Amorphous materials Inc. Solvents N, N-dimethyl formamide (DMF) and acetone were obtained from Alfa Aesar and BDH, respectively. MWCNTs (90% purity, ~9.5 nm diameter and ~1.5 μm length) produced by catalytic carbon vapor deposition under the brand name NC-7000 were procured from Nanocyl™.

2.2 Polymer solution preparation

Printable ink design: A mixture of acetone and dimethyl formamide (DMF) was chosen as the solvent system for PVDF as in most electrospinning processes [27]. DMF is considered the least hazardous amongst the solvents used for PVDF while acetone has a low evaporation point (~56 °C). The boiling point of DMF is around 153 °C [28]. The ratio of DMF:acetone was experimentally optimized to 40:60 to use least amount of DMF and achieve the desired printing performance. Dimethyl sulfoxide (DMSO) was added as a β-phase initiating agent [21].

Various concentrations (15-30 wt.%) of PVDF in DMF:acetone mixture were studied for their printability. 20 wt.% of PVDF in the solution-mixture, with viscosities lower than 10 Pa-s, was observed to be the best to print 2D films, higher concentrations around (viscosities close to 100 Pa-s) were found to be convenient to form 3D structures. The solutions were prepared via ultrasonication of PVDF powder with the solvent-mixture. A solution cast film was also prepared using 20 wt.% PVDF solution for comparison.

Nanocomposite formulation: MWCNTs were oxidised by refluxing in a mixture of nitric and sulphuric acid in 1:3 ratio at 70 °C for 7 h. This was followed by repeated washing to remove the acid [29]. 0.25, 0.5 and 1.0 wt.% of MWCNTs were dispersed in acetone for 3 h via ultrasonication. Later PVDF, DMF and DMSO were added and the solution was further ultrasonicated for 20 minutes.

To prepare the BTN/PVDF nanocomposites 1.0 wt.% BTNs were added to DMF and ultrasonicated for 3 h. DMF was used because of its ability to completely dissolve BTNs [30]. The nanoparticle solution was later ultrasonicated with a mixture of PVDF and acetone followed by the addition of DMSO.

2.3 Printing

PVDF and its nanocomposite solutions (further referred to as 'inks') were poured into 3 cc syringe barrels to enable printing. The syringe barrels were placed into a pneumatically operated dispensing system (HP-7X, EFD) to apply precise pressures for deposition. A robotic head (I&J2200-4, I&J Fisnar Inc.), controlled by a commercial software (JR Points for Dispensing, Janome Sewing Machine) further enabled the deposition of the inks on a movable flat stage. 1D filaments, 2D films and 3D self-supporting structures were fabricated from different solution concentrations (20 wt.% - 25 wt.%), varying extrusion pressures, *P* (100 to 1500 kPa) and nozzles (i.e., inner diameter = 100 to 330 µm) on an aluminium substrate. Table 1 shows the type and amount of filler added to PVDF and the nozzle diameter used to print the nanocomposite films. Different concentrations of fillers in the nanocomposite solutions lead to different viscosities. This demanded the use of nozzles with different diameters for printing.

Sample code	Filler	Filler Concentration (wt. %)	Nozzle diameter (µm)
PVDF	-	-	100
0.25MWCNT/PVDF	MWCNTs	0.25	150
0.5 MWCNT/PVDF	MWCNTs	0.5	250
1MWCNT/PVDF	MWCNTs	1.0	330
1BTN/PVDF	BTNs	1.0	100

Table 1: Filler concentration and printing parameters of PVDF and its nanocomposite films

2.3 Characterization

The effect of PVDF filler type, shear stress (extrusion pressure) and shear rate (printing speed) on the apparent viscosity of PVDF solutions was studied with the help of capillary flow analysis and apparent viscosity tests as previously developed by Bruneaux *et al*. [31]. Apparent flow rates and viscosities of the solutions at the instant of printing were studied by depositing known lengths of polymer filaments using a 100 µm diameter nozzle at various extrusion pressures. A weighing scale (GH200, A&D) was used to determine the mass of the fibers after complete evaporation of the solvents. Five fibers were printed at each pressure for every solution.

FTIR – Photo acoustic spectroscopy (FTS 6000 spectrometer, Bio-rad) was used to obtain the absorption spectra of PVDF and its nanocomposite films in the range of 400 – 4000 cm^{-1}. A Philips X'pert diffractometer was used with scan angles from 15 to 30° at room temperature to obtain the diffractogram patterns of the films. A scan rate of 0.4 $°min^{-1}$ was used with a Cu target and K_α radiation at 50 kV and 40 mA.

Optical microscopy (BX-61 Olympus; Image-Pro plus V5 an image processing software from Media Cybernetics) was used to study the thicknesses and morphology of structures 3D printed with

PVDF and nanocomposites. The morphology of the 3D printed films was observed using a JEOL JSM-7600TFE field emission scanning electron microscope (FESEM) at 10 kV.

Impedance tests to determine the dielectric constant and capacitance were performed using an Agilent 4294A Precision impedance analyser in the frequency range of 40 to 110 MHz.

3 RESULTS AND DISCUSSION

1D fibers (Figure 1a), 2D films (Figure 1b) and 3D scaffolds (Figure 1c) were successfully fabricated using different concentrations of PVDF in DMF:Acetone mixture. The printing parameters are provided in the legends. 1D fibers with circular cross-section were printed using 25 wt.% PVDF solution and 100 µm nozzle. The inset on the top-right of Figure 1a shows the circular cross section of the fiber with an average diameter of 55 µm. The diameter of the fiber is lower than the nozzle size due to the evaporation of the solvent post extrusion. Films were fabricated with 20 wt.% and a 100 µm nozzle to print as thin films as possible. The printed PVDF films were continuous, smooth, gap-free and 130 µm thick. A 8-layered scaffold were fabricated using 22.5 wt.% PVDF to demonstrate the 3D printability of PVDF. Successful fabrication of layer-by-layer structures on flat surfaces has been demonstrated. Higher concentrations of PVDF need to be investigated in order to form complex free-standing 3D geometries.

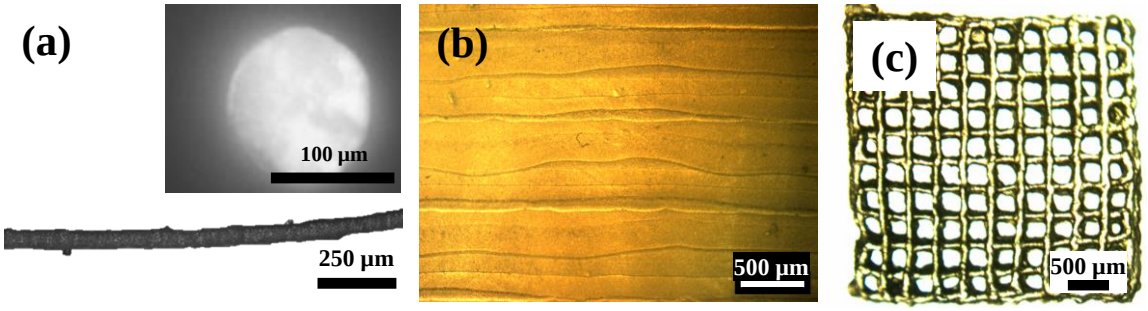

Figure 1: (a) 1D fiber (Nozzle = 100 µm, 25 wt.% PVDF); (b) 2D film (Nozzle = 100 µm, 20 wt.% PVDF); (c) 3D scaffolds printed (Nozzle =100 µm, 22.5 wt.% PVDF)

After investigating the piezoelectric properties of all the MWCNT/PVDF nanocomposites, it was found that 1MWCNT/PVDF had the best piezoelectric properties. Hence, 1BTN/PVDF solution was prepared and compared for its printability and piezoelectricity with 1MWCNT/PVDF. PVDF, 1MWCNT/PVDF and 1BTN/PVDF fibers and films were fabricated using 20 wt.% PVDF solutions and tested for the effect of filler concentration and filler type on 3D printing.

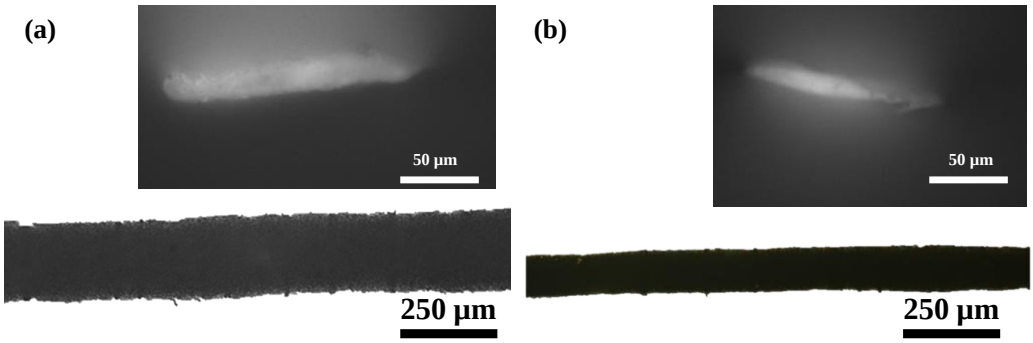

Figure 2: Microscopic images of fibers printed using (a) 1MWCNT/PVDF; (b) 1BTN/PVDF; (Nozzle = 100 µm, *P* = 280 kPa). The insets on the top-right are the cross-sections of the fibers.

Figure 2a and 2b are the microscopic images of 1MWCNT/PVDF and 1BTN/PVDF fibers printed

using 100 µm nozzles at 280 kPa. The 1MWCNT/PVDF fibers were grey in color while the 1BTN/PVDF fibers had a milky-white appearance. The fibers printed with 20 wt.% PVDF nanocomposite solutions were not circular in cross-section as in Figure 1a because of their deposition on a flat substrate with a lower viscosity. The 1MWCNT/PVDF had a width of about 200 µm and a thickness of 18 µm. The 1BTN/PVDF was about 110 µm wide and 12 µm thick. To form PVDF fibers with circular circular cross-section a much higher viscosity as in 25 wt.% PVDF solutions is required.

3D printability from a polymer solution is mainly governed by the viscosity and evaporation rate. The viscosity of the polymer solution changes when subjected to different extrusion pressures and printing speeds. To determine the effect of PVDF and nanofillers' concentration on this apparent viscosity, pressure-assisted printability of the polymer and its nanocomposite inks was investigated. Fibers from PVDF, 1MWCNT/PVDF and 1BTN/PVDF inks were printed at different extrusion pressures using 100 µm nozzles. Figure 3a shows the variation of the volumetric flow rate of the three solutions with respect to the applied pressures. The slope of the curves gives the estimate of shear thinning behaviour of the solutions. There is a linear increase in the flow rates of the solution with the increase in applied pressure.

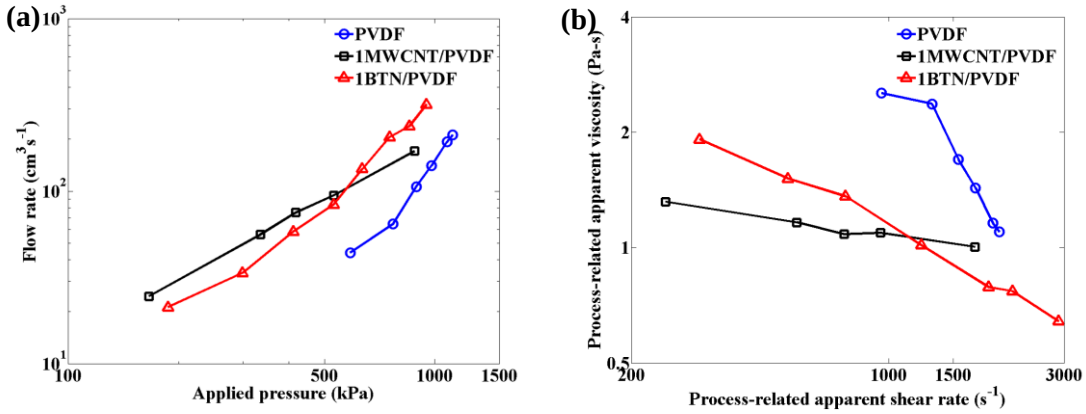

Figure 3: (a) Volumetric flow rate versus applied pressure while printing PVDF based fibers (b) Process-related apparent viscosity as a function of process-related apparent shear rate. (Nozzle diameter = 100 µm; *P* = 100-1500 kPa)

Figure 3b shows the variation of process-related viscosities at different shear rates. A decrease in apparent viscosity with increasing shear rates can be observed. The shear thinning index given by the logarithmic ratio of shear stress by shear rate [26], is higher for 1BTN/PVDF (1.72) than that for 1MWCNT/PVDF (1.05). The shear thinning index of neat PVDF (2.64) is much higher than both the nanocomposites. This implies that neat PVDF and 1BTN/PVDF had a higher decrease in viscosity with the increase in shear rates, but 1MWCNT/PVDF showed a lower degree of shear thinning in the same shear rate range. The highest viscosity available for the solutions at this filler and polymer concentration is about 3 Pa-s which is a good value for the printing films. Lower viscosity in case of the nanocomposites is attributed to phase separation due to inhomogenous mixing in the inks. This phenomenon needs to be further studied. Lower viscosity of the 1MWCNT/PVDF ink can be the reason for a larger size of the 1MWCNT/PVDF fiber in Figure 2a as compared to the 1BTN/PVDF in Figure 2b. Higher viscosities will be required for printing 3D shapes as lower solvent concentration will facilitate faster evaporation aiding the retention of 3D geometries. Also, the 1MWCNT/PVDF ink due to inhomogeneous mixing of fillers in the solution, posed clogging issues while printing.

The phase characterisation of the PVDF and its nanocomposite films fabricated at 1000 kPa (printing nozzle diameters as per Table 1) was carried out using FTIR and XRD techniques. The FTIR spectra in Figure 4a, show spectral bands at 763 cm^{-1} for α-phase and 510 and 840 cm^{-1} for β-phase [32]. There is an increase in the content of β-phase in the case of 3D printed films as signified by lower transmittance at 840 cm^{-1}. Within the 3D printed films the nanocomposite films contain higher β-phase as compared to the neat PVDF film. The presence of spectral bands at 490, 615 and 763 cm^{-1} [33] depicts that α-phase still coexists in the material. Spectral bands corresponding to γ-phase around 776 and 812 cm^{-1} were not visible.

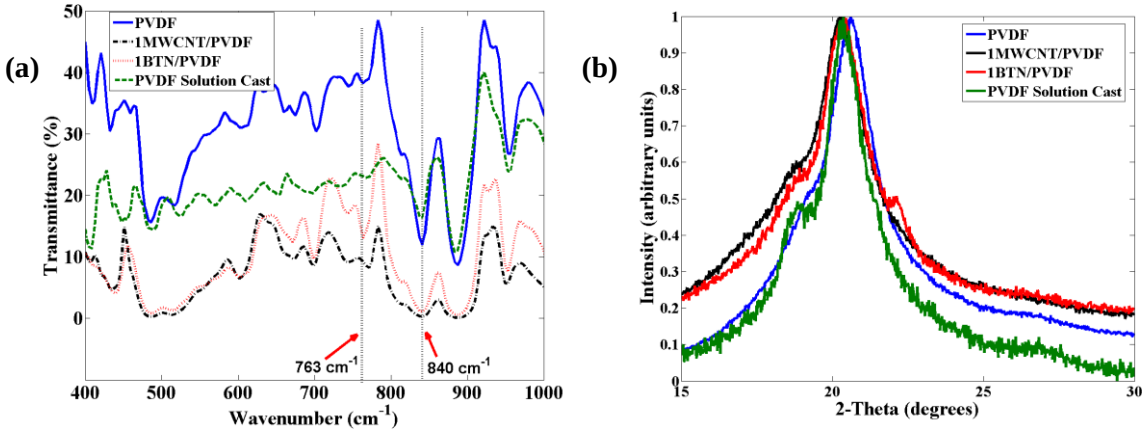

Figure 4: (a) FTIR spectra (b) X-ray diffractograms of PVDF and nanocomposite films

Figure 4b shows the X-ray diffractograms of solution cast and 3D printed neat PVDF films and 3D printed nanocomposites. In case of the solution cast film distinct peaks at 18.5, 20.1 and 26.7° belonging to α-phase are analogous with those found in literature [34]. There is a complete disappearance of the α-peak at 26.5° in all the 3D printed films. This is because of the additional shearing and stretching taking place during the printing process [20]. Peak broadening at 20.5° [32] attributing to the increase in β-phase of PVDF is evident in the nanocomposites. The increase in β-phase content is because of the retention of the β-chains by the heavy filler molecules.

Figure 5a to 5c show the FESEM image of neat PVDF, 1MWCNT/PVDF and 1BTN/PVDF films fabricated at 1000 kPa. To form sensors it is important to obtain smooth films free from pores [35]. There are microscopic pores present in all the films, formed due to the evaporation of the solvents. Larger pore sizes are due to lower solvent evaporation rates [36]. The pore size is the smallest in case of 1BTN/PVDF (2-3 μm), and is larger in the case of 1MWCNT/PVDF (6-7 μm). Some fibrous networks are seen in 1MWCNT/PVDF which are absent in the other two films.

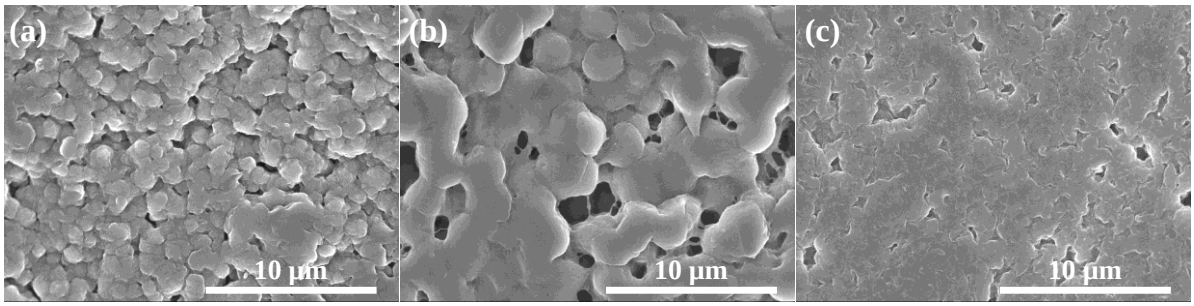

Figure 5: FESEM images showing the surface texture of 3D printed films (P = 1000 kPa) (a) Neat PVDF (Nozzle = 330 μm); (b) 1MWCNT/PVDF (Nozzle = 330 μm); (c) 1BTN/PVDF (Nozzle = 100 μm)

Samples for impedance measurements were prepared by silver painting electrodes over a circular area of 7 mm diameter. Impedance values obtained from the Impedance analyser were used to calculate the dielectric constant and capacitances of neat PVDF and nanocomposite sensors. The dielectric constant and capacitances of the PVDF sensors are shown in Table 2. The dielectric constant of neat PVDF was between 8 and 10, as found in the literature [37, 38]. This confirms that 3D printing is not harming the piezoelectric properties in PVDF. There is an increase in the dielectric constant of the films upon addition of the fillers. The capacitance of 1BTN/PVDF is found to be three times that obtained with neat PVDF film. Dielectric constant of 20 in 1BTN/PVDF is a high value for such a low loading of BTNs. It usually requires higher percentages (eg. 20 wt.% [37]) of BTNs in PVDF to have a

dielectric constant values close to 20 [37, 39, 40].

Sensor	Thickness (μm)	Dielectric constant	Capacitance (pF)
PVDF	130	9	24
1MWCNT/PVDF	350	64	60
1BTN/PVDF	85	20	79

Table 2: Impedance test results: Dielectric constant and capacitance along with the thicknesses of the films

The results from the impedance tests shown in Table 2 exhibit 1MWCNT/PVDF film had higher dielectric constant compared to the 1BTN/PVDF sensor. But the ability to print considerably thinner films (utilizing smaller nozzle sizes) makes BTN nanocomposite a better candidate for piezoelectric applications.

The major challenge in this work was to attain high piezoelectric properties in the 3D printed PVDF, which usually requires cumbersome post processing treatments like annealing [5], stretching [41] and poling [42]. Addition of fillers led to an improvement in the piezoelectric properties of PVDF. MWCNTs though had a considerable effect on the properties of PVDF, they posed problems of inhomogeneous mixing and hence, led to difficulties in the printing process with 100-250 μm nozzles. BTNs already being piezoelectric not only did perform better than PVDF but also exhibited potential scope for printing due to their better shear thinning behavior as compared to MWCNTs. PVDF nanocomposites performed better than neat PVDF and their properties are comparable to those found in literature. Incorporation of higher percentages of fillers into the PVDF matrix with homogenous mixing needs to be pursued to attain dielectric constant values close to piezoelectric ceramics.

5 CONCLUSIONS

Successful 3D printability was demonstrated with PVDF and its nanocomposite solutions with MWCNTs and BTNs. 3D printed PVDF films had higher content of β-phase than the solution cast ones. Addition of fillers significantly improved the piezoelectric properties of the PVDF sensors. The dielectric constant of BTN/PVDF was higher than that found in the literature. The capacitance of the BTN/PVDF film was three times higher than the neat PVDF film. BTNs proved to be convenient filler options than MWCNTs due to the ease in printing as well as better piezoelectric properties. The next step will be to print piezoelectric sensors using BTN/PVDF nanocomposites directly on the structures and study the piezoelectric charge and force constants of the material.

ACKNOWLEDGEMENTS

The authors acknowledge the financial support from NSERC (National Sciences and Engineering Research Council of Canada) and CFI (Canadian Foundation for Innovation).

REFERENCES

1. Lando, J.B. and W.W. Doll, *The polymorphism of poly(vinylidene fluoride). I. The effect of head-to-head structure.* Journal of Macromolecular Science, Part B, 1968. **2**(2): p. 205-218.
2. Sessler, G.M., *Piezoelectricity in polyvinylidenefluoride.* The Journal of the Acoustical Society of America, 1981. **70**(6): p. 1596-1608.
3. Ye, Y.U.N., et al., *Phase transitions of poly(vinylidine fluoride) under electric fields* Integrated Ferroelectrics, 2006. **80**(1): p. 245-251.
4. Chung, M.Y.L., D. C., *Electrical Properties of Polyvinylidene Fluoride Films Prepared by the High Electric Field Applying Method.* Journal of the Korean Physical Society, 2001. **38**(2): p. 6.

5. Seok Ju, K., et al., *Spin cast ferroelectric beta poly(vinylidene fluoride) thin films via rapid thermal annealing.* Applied Physics Letters, 2008. **92**(1): p. 012921-012921-3.
6. Theron, S.A., E. Zussman, and A.L. Yarin, *Experimental investigation of the governing parameters in the electrospinning of polymer solutions.* Polymer, 2004. **45**(6): p. 2017-2030.
7. Yee, W.A., et al., *Morphology, polymorphism behavior and molecular orientation of electrospun poly(vinylidene fluoride) fibers.* Polymer, 2007. **48**(2): p. 512-521.
8. Liu, Y., et al., *Effects of Drawing Temperature on Phase Transition in Poly(Vinylidene Fluoride) Films.* Ferroelectrics, 2002. **273**(1): p. 3-8.
9. Huang, W., et al., *Nanocomposites of poly(vinylidene fluoride) with multiwalled carbon nanotubes.* Journal of Applied Polymer Science, 2010. **115**(6): p. 3238-3248.
10. Liu, Z.H., et al., *Piezoelectric properties of PVDF/MWCNT nanofiber using near-field electrospinning.* Sensors and Actuators A: Physical, 2013. **193**(0): p. 13-24.
11. Dillon, D.R., et al., *On the structure and morphology of polyvinylidene fluoride–nanoclay nanocomposites.* Polymer, 2006. **47**(5): p. 1678-1688.
12. Rajesh, P.S.M., et al., *Enhancing beta-phase in PVDF through physicochemical modification of cellulose.* Electronic Materials Letters, 2014. **10**(1): p. 315-319.
13. Andrew, J.S. and D.R. Clarke, *Enhanced Ferroelectric Phase Content of Polyvinylidene Difluoride Fibers with the Addition of Magnetic Nanoparticles.* Langmuir, 2008. **24**(16): p. 8435-8438.
14. Jing, X., et al., *Magnetic and dielectric properties of barium ferrite fibers/poly(vinylidene fluoride) composite films.* Journal of Polymer Research, 2011. **18**(6): p. 2017-2021.
15. El Achaby, M., et al., *Nanocomposite films of poly(vinylidene fluoride) filled with polyvinylpyrrolidone-coated multiwalled carbon nanotubes: Enhancement of β-polymorph formation and tensile properties.* Polymer Engineering & Science, 2013. **53**(1): p. 34-43.
16. Martins, P., C.M. Costa, and S. Lanceros-Mendez, *Nucleation of electroactive β-phase poly(vinilidene fluoride) with CoFe2O4 and NiFe2O4 nanofillers: a new method for the preparation of multiferroic nanocomposites.* Applied Physics A, 2011. **103**(1): p. 233-237.
17. Corral-Flores, V., et al., *Preparation of Electrospun Barium Titanate – Polyvinylidene Fluoride Piezoelectric Membranes.* Materials Science Forum, 2010. **644**: p. 33-37.
18. He, L., et al., *Enhancement of β-crystalline phase of poly(vinylidene fluoride) in the presence of hyperbranched copolymer wrapped multiwalled carbon nanotubes.* Journal of Colloid and Interface Science, 2011. **363**(1): p. 122-128.
19. Wang, S.-H., et al., *Mechanical and electrical properties of electrospun PVDF/MWCNT ultrafine fibers using rotating collector.* Nanoscale Research Letters, 2014. **9**(1): p. 522-522.
20. Yu, H., et al., *Enhanced power output of an electrospun PVDF/MWCNTs-based nanogenerator by tuning its conductivity.* Nanotechnology, 2013. **24**(40): p. 405401.
21. Benz, M., W.B. Euler, and O.J. Gregory, *The Role of Solution Phase Water on the Deposition of Thin Films of Poly(vinylidene fluoride).* Macromolecules, 2002. **35**(7): p. 2682-2688.
22. Seoul, C., Y.-T. Kim, and C.-K. Baek, *Electrospinning of poly(vinylidene fluoride)/dimethylformamide solutions with carbon nanotubes.* Journal of Polymer Science Part B: Polymer Physics, 2003. **41**(13): p. 1572-1577.
23. Sun, D., et al., *Near-Field Electrospinning.* Nano Letters, 2006. **6**(4): p. 839-842.
24. Pu, J., et al., *Piezoelectric actuation of direct-write electrospun fibers.* Sensors and Actuators A: Physical, 2010. **164**(1–2): p. 131-136.
25. Guo, S.Z., et al., *Solvent-cast three-dimensional printing of multifunctional microsystems.* Small, 2013. **9**(24): p. 4118-22.
26. Guo, S.-Z., M.-C. Heuzey, and D. Therriault, *Properties of Polylactide Inks for Solvent-Cast Printing of Three-Dimensional Freeform Microstructures.* Langmuir, 2014. **30**(4): p. 1142-1150.
27. Koombhongse, S., W. Liu, and D.H. Reneker, *Flat polymer ribbons and other shapes by electrospinning.* Journal of Polymer Science Part B: Polymer Physics, 2001. **39**(21): p. 2598-2606.
28. *A13547 N,N-Dimethylformamide, 99%,* A.A. (R), Editor.

29. Dang, Z.-M. *High Dielectric Constant Percolative Nanocomposites Based on Ferroelectric Poly(vinylidene fluoride) and Acid-Treatment Multiwall Carbon Nanotubes*. in *Properties and applications of Dielectric Materials, 2006. 8th International Conference on*. 2006.
30. Corral-Flores, V. and D. Bueno-Baqués, *Flexible Ferroelectric BaTiO3 – PVDF Nanocomposites*. Ferroelectrics - Material Aspects2011.
31. Bruneaux, J., D. Therriault, and M.-C. Heuzey, *Micro-extrusion of organic inks for direct-write assembly.* Journal of Micromechanics and Microengineering, 2008. **18**: p. 11.
32. Martins, P., A.C. Lopes, and S. Lanceros-Mendez, *Electroactive phases of poly(vinylidene fluoride): Determination, processing and applications.* Progress in Polymer Science, (0).
33. Shah, D., et al., *Dramatic Enhancements in Toughness of Polyvinylidene Fluoride Nanocomposites via Nanoclay-Directed Crystal Structure and Morphology.* Advanced Materials, 2004. **16**(14): p. 1173-1177.
34. Buckley, J., et al., *Nanocomposites of poly(vinylidene fluoride) with organically modified silicate.* Polymer, 2006. **47**(7): p. 2411-2422.
35. Cardoso, V.F., et al., *Micro and nanofilms of poly(vinylidene fluoride) with controlled thickness, morphology and electroactive crystalline phase for sensor and actuator applications.* Smart Materials and Structures, 2011. **20**(8): p. 087002.
36. Magalhães, R., et al., *The Role of Solvent Evaporation in the Microstructure of Electroactive β-Poly(Vinylidene Fluoride) Membranes Obtained by Isothermal Crystallization.* Soft Materials, 2010. **9**(1): p. 1-14.
37. Li, Y.C., S.C. Tjong, and R.K.Y. Li, *Dielectric properties of binary polyvinylidene fluoride/barium titanate nanocomposites and their nanographite doped hybrids.* Express Polymer Letters, 2011.
38. Dang, Z.M., et al., *Dielectric behavior of novel three-phase MWNTs/BaTiO3/PVDF composites.* Materials Science and Engineering: B, 2003. **103**(2): p. 140-144.
39. Zhang, L., D. Xiao, and J. Ma, *Dielectric Properties of PVDF/Ag/BaTiO3 Composites.* Ferroelectrics, 2013. **455**(1): p. 77-82.
40. Song, Y., et al., *Enhanced dielectric and ferroelectric properties induced by dopamine-modified BaTiO3 nanofibers in flexible poly(vinylidene fluoride-trifluoroethylene) nanocomposites.* Journal of Materials Chemistry, 2012. **22**(16): p. 8063-8068.
41. Sajkiewicz, P., A. Wasiak, and Z. Gocłowski, *Phase transitions during stretching of poly(vinylidene fluoride).* European Polymer Journal, 1999. **35**(3): p. 423-429.
42. *Poling and characterization of piezoelectric polymer fibers for use in textile sensors.* Sensors and Actuators A: Physical, 2013.